Eye (2019) 33:1240–1247
https://doi.org/10.1038/s41433-019-0401-7

The ROYAL COLLEGE of OPHTHALMOLOGISTS

ARTICLE

Macular OCT-angiography parameters to predict the clinical stage of nonproliferative diabetic retinopathy: an exploratory analysis

Tiago M. Rodrigues[1,2,5] · João P. Marques[1,3,4] · Mário Soares[1] · Sílvia Simão[3] · Pedro Melo[1] · Amélia Martins[1] · João Figueira[1,3,4] · Joaquim N. Murta[1,3,4] · Rufino Silva[1,3,4]

Received: 11 November 2018 / Accepted: 18 February 2019 / Published online: 22 March 2019

Abstract

Background To test whether a single or a composite set of macular vascular density parameters, evaluated with optical coherence tomography angiography (OCTA), are able to predict nonproliferative diabetic retinopathy (NPDR) staging according to the gold-standard ETDRS-grading scheme.

Methods Prospectively defined, cross-sectional study in which macular structural and vascular parameters of diabetic eyes with nonproliferative DR (up to ETDRS Level 53) were evaluated with OCTA (Avanti RTVue-XR 100, Optovue Inc, Fremont, CA). Seven-field photographs of the fundus were taken for DR staging according to the ETDRS-grading scheme. The vessel density in the superficial and deep capillary plexus (SCP and DCP, respectively), as well as in the choriocapillaris (CC), were calculated using automated software. Univariate and multivariate ordered logistic regression models were used in the analysis. $P < 0.05$ was considered statistically significant.

Results We included 101 eyes from 56 subjects (mean (SD) age 62.64 (11.74) years; 57.4% were male). On univariate analysis, several OCTA parameters were found to be associated with higher ETDRS level (parafoveal SCP density: OR = 0.87 (95% CI 0.76–0.99), $p = 0.039$; parafoveal DCP density: OR = 0.79 (95% CI 0.72–0.87), $p < 0.001$; CC density: OR = 0.89 (95% CI 0.80–0.99)), $p = 0.036$). In the final model, while also adjusting for relevant clinical features, only parafoveal vessel density in the DCP remained as a significant predictor of NPDR ETDRS level (OR = 0.54 (95% CI 0.32–0.92), $p = 0.024$).

Conclusion Our results suggest that parafoveal vessel density in the DCP is the parameter most robustly associated with ETDRS level. OCTA analysis may provide objective imaging biomarkers to monitor NPDR clinical progression.

Supplementary information The online version of this article (https://doi.org/10.1038/s41433-019-0401-7) contains supplementary material, which is available to authorized users.

✉ Tiago M. Rodrigues
tiago.fm.rod@gmail.com

1 Department of Ophthalmology, Centro Hospitalar e Universitário de Coimbra – CHUC, E.P.E. Praceta Professor Mota Pinto, 3000-075 Coimbra, Portugal

2 Instituto de Medicina Molecular, Faculdade de Medicina, Universidade de Lisboa, Avenida Professor Egas Moniz, 1649-028 Lisboa, Portugal

3 Association for Innovation and Biomedical Research on Light and Imaging (AIBILI), Azinhaga de Santa Comba, 3000-548 Coimbra, Portugal

4 Faculty of Medicine, University of Coimbra (FMUC), Rua Larga, 3004-204 Coimbra, Portugal

5 Present address: Institute of Molecular and Clinical Ophthalmology Basel (IOB), Mittlere Strasse 91, CH-4031 Basel, Switzerland

Introduction

Diabetic retinopathy (DR) is already one of the leading causes of blindness worldwide [1] and the prevalence of vision-threatening DR is expected to double in the next decade [2]. Considering that > 90% of cases of vision loss can be prevented [3], accurate staging and classification of DR are paramount to guide treatment decisions and determine prognosis.

The Early Treatment of Diabetic Retinopathy Study (ETDRS) grading scheme is the gold-standard for DR staging [4]. However, it is labor-intensive, low-throughput and, thus, has limited applicability for population-wide screening and staging.

Optical Coherence Tomography Angiography (OCTA) provides non-invasive, three-dimensional mapping of the retina and choroidal microvasculature [5]. Both qualitative vascular abnormalities [6] and quantitative measurements

[7–9] were shown to correlate with clinical features of DR, across its main stages. In this sense, efforts were made to implement OCTA-based methods for high-throughput DR detection [10]. Although OCTA-based approaches seem able to detect DR (versus no-DR) and to differentiate between DR main clinical stages (nonproliferative vs. proliferative), the capacity of OCTA to discriminate between substages, i.e., within the nonproliferative spectrum, is less clear.

Therefore, in this study, we aimed to directly confront ETDRS grading (the gold-standard) with automated, built-in software-driven OCTA parameters, to determine whether any single or composite set of these is predictive of nonproliferative diabetic retinopathy (NPDR) ETDRS level.

Methods

Study participants

This is a hospital-based, cross-sectional, observational cohort study, conducted at the Department of Ophthalmology of Centro Hospitalar e Universitário de Coimbra (CHUC). The study was approved by the local Ethics Committee. All participants gave oral and written informed consent. Recruitment occurred between October 2017 and March 2018.

We included consecutive adult patients (>18 years old) diagnosed with either type 1 or type 2 DM. Patients presenting proliferative DR (ETDRS Level 61 or higher) or macular edema were excluded. Likewise, (i) high ametropias (spherical equivalent > 6 D), (ii) ocular hypertension or glaucoma, (iii) previous laser retina treatment and/or intravitreal injection, (iv) any other retinal or choroidal disorder (e.g., AMD), and (v) any media opacities likely to compromise image acquisition and/or interpretation were defined as exclusion criteria.

Clinical evaluation

First, we collected demographic data, including: (i) age; (ii) gender; (iii) known systemic and ocular disorders; (iv) previous systemic and ocular treatments; and (v) current and previous medication. Second, blood was drawn for glycosylated hemoglobin (HbA1c) analysis. Third, we performed a full bilateral ophthalmologic examination, including (i) subjective refraction and distance best-corrected visual acuity using a modified ETDRS chart with Sloan Letters (Cat. No. L220, Lighthouse Enterprises, NY, USA); (ii) intraocular pressure measurement with a Goldmann tonometer; (iii) anterior segment biomicroscopy and dilated fundus examination.

ETDRS grading

Seven standard 45°-field photographs of the eye fundus were taken with a Nikon Digital SLR Camera D7000 (Nikon Corporation, Japan) mounted on a TRC-NW7SF Mark II Retinal Camera (TopCon Corporation, Japan) by certified orthoptic technicians (M.S. and P.M.), and stored on a computer. ETDRS staging was later performed, according to the Modified Airlie-House Classification [4], by one grader (S.S.) certified by the Coimbra Ophthalmology Reading Center (CORC), who was fully blinded to all study variables.

OCTA image acquisition and analysis

OCTA images were obtained with a commercial spectral-domain OCT system (Avanti RTVue-XR 100, Optovue Inc, Fremont, CA, USA). Each subject underwent a single imaging session that included two scans over a 3 × 3-mm region centered in the fovea. Details regarding physical properties of the scan and sampling rate are provided elsewhere [7]. The split-spectrum amplitude-decorrelation angiography algorithm was used to compute a flow map for each scan, as previously described [5]. The Motion Correction Technology (MCT) of Optovue software was used to compensate for motion artifacts [11]. Images with inadequate signal strength due to motion or low signal strength (< 6/10) were excluded from the analysis.

Retinal layers were segmented between the inner limiting membrane (ILM) and the retinal pigment epithelium (RPE) on the basis of OCT structural image. An en face OCT angiogram was, then, produced by maximum decorrelation (flow) projection within the segmented retina. We included three layers from the en face OCT angiogram in our analysis: the superficial capillary plexus (SCP), the deep capillary plexus (DCP) and the choriocapillaris (CC). The built-in software (AngioVue version 2017.1.0.116; Optovue Inc, Fremont, CA) automatically segments these vessel layers. SCP consists of capillaries between the ILM and posterior boundary of the inner plexiform layer (IPL) (including the nerve fiber and ganglion cell layers). The DCP consists of capillaries between the posterior boundary of the IPL and the posterior boundary of the outer plexiform layer (OPL) (including the inner nuclear layer). Finally, the CC consists of capillaries in a 30-μm-thick layer posterior to the RPE-Bruch membrane junction. The OCT system's software automatically computes the vessel density within the entire scan (total density) and within the annular zone of 1- to 3-mm diameter around the foveal center (parafoveal density) of both the SCP and DCP scans, as well as the area of the foveal avascular zone (FAZ). Vessel density in the CC slab was determine after binarization using the Otsu method [12]. Average macular ganglion cell complex

(GCC) thickness, central retinal thickness, total retinal volume, parafoveal (within a 3-mm-diameter centered in the foveal) retinal volume and thickness were all analyzed with OCT (Avanti RTVue-XR 100, Optovue Inc, Fremont, CA, USA), using the built-in software.

Statistical analysis

As this is an exploratory analysis, no sample size calculations were performed. The target size of our sample was based on previous reports [6–9].

The study population demographics, clinical and imaging characteristics were summarized using traditional descriptive methods. For this purpose, the sample was stratified into 4 levels, according to ETDRS grading (Level 10, 20, 35, and 43 + 47). Thus, some of the original sublevels were grouped together (e.g., 35 C, 35D, 35E, and 35 F are all within the Level 35 stratum). Pearson product–moment correlation coefficients were used to explore the association between vascular OCTA features and also between vascular and structural parameters.

In order to test which clinical and imaging features were predictive of ETDRS grading (the outcome), we built ordered logistic regression (OLR) models. In these models, to be conservative, no sublevel grouping was performed. Thus, the outcome retained 9 ordinal levels, i.e., the number of distinct ETDRS stages included in our sample (ETDRS Levels 10, 20, 35 C, 35D, 35E, 35 F, 43 A, 43B, 47 A). Robust standard errors were calculated while clustering on patient-level, to adjust for intrapatient correlation (since both eyes of the same patient were included whenever possible). For model building, we first conducted a univariate OLR analysis for each predictor. All variables with a $P < 0.10$ were subsequently included in the multivariate model, to control for potential confounders. The final model was built from the multivariate model through a step-down approach. Odds Ratios (OR) are reported with 95% confidence intervals (CI). In order to verify the proportional odds assumption (and, thus, the validity of the final model), a Brant's test was performed. A receiver operating characteristic (ROC) curve analysis was conducted to assess the discriminative ability of the final model for different ETDRS cutoff levels. Larger areas under the ROC curve (C-statistic) indicate higher discriminative capacity. Finally, as a sensitivity analysis, we applied the same model building strategy outlined above to predict the outcome, considering only 4 levels (i.e., the same levels used for the descriptive analysis).

All statistics were performed on STATA (version 14.2, StataCorp LCC, College Station, TX, USA). Graphical representations were built either on STATA or R studio (version 1.1.477), with the ggplot2 package [13]. $P < 0.05$ was considered statistically significant.

Results

Demographic and clinical characteristics

We imaged and analyzed a total of 116 eyes of 58 patients; after exclusion criteria were applied, 101 eyes of 56 patients were considered for analysis. Reasons for exclusion were as follows: branch retinal artery occlusion ($n = 4$), branch retinal vein occlusion ($n = 3$), proliferative DR ($n = 3$), macular edema ($n = 2$) and poor-quality scan ($n = 3$). The percentage of missing data in our data set is 0.7%.

The ETDRS grading of the 101 eyes included was the following: Level 10, $n = 19$; Level 20, $n = 28$; Level 35 C, $n = 23$; Level 35D, $n = 15$; Level 35E, $n = 3$; Level 35 F, $n = 4$; Level 43 A, $n = 3$; Level 43B, $n = 4$; Level 47 A, $n = 2$. For the descriptive analysis, eyes were grouped in four strata, as follows: Level 10 ($n = 19$), Level 20 ($n = 28$), Level 35 ($n = 45$), and Level 43 + 47 ($n = 9$).

Demographic and clinical characteristics of these groups are summarized in Table 1. As expected, the average level of HbA1C, time since the diagnosis of DM and prevalence of insulin use all increase with advancing stages of NPDR.

Descriptive analysis of OCT parameters

The mean values (± SD) of macular structural and vascular features are presented in Table 2. Crude analysis of these values elucidates no clear trends for structural parameters. However, vessel density in the SCP, DCP, and CC tend to decrease, in the more-advanced stages of NPDR.

The correlation analysis shows that, in diabetic patients, parafoveal SCP and DCP density are moderately correlated ($R = 0.259$, $p = 0.009$; Fig. 1a), but only the latter was found to be negatively correlated with FAZ ($R = -0.302$, $p = 0.002$; Fig. 1b, c). Regarding neurovascular associations, GCC thickness and SCP density were found to be significantly correlated ($R = 0.375$, $p < 0.001$; Fig. 1d). Furthermore, DCP (but not SCP) density correlates negatively with parafoveal retinal thickness ($R = -0.302$, $p = 0.002$; Fig. 1e, f) and volume ($R = -0.242$, $p = 0.016$; Fig. 1g, h).

OCT parameters as predictors of NPDR ETDRS level

On univariate analysis, several OCTA parameters were found to be associated with NPDR progression, including vascular density in the CC (OR = 0.89 (0.80, 0.99), $p = 0.036$), as well as in parafoveal SCP (OR = 0.87 (0.76, 0.99), $p = 0.039$) and DCP (OR = 0.79 (0.72, 0.87), $p < 0.001$). In contrast, even on univariate analysis, none of the structural outcomes studied was a significant predictor of the ETDRS level (Table 3). Concomitant diagnosis of systemic

Table 1 Demographic and clinical characteristics of study eyes

	ETDRS level				Total ($n = 101$)
	Level 10 ($n = 19$)	Level 20 ($n = 28$)	Level 35 ($n = 45$)	Levels 43/47 ($n = 9$)	
Age, years	66.79 ± 12.24	57.86 ± 12.43	62.60 ± 11.03	69.00 ± 5.32	62.64 ± 11.74
Sex (male), prevalence	11/19 (57.9%)	14/28 (50%)	31/45 (68.9%)	2/9 (22.2%)	58/101 (57.4%)
SAH, prevalence	14/19 (73.7%)	23/28 (82.1%)	43/45 (95.6%)	8/9 (88.9%)	88/101 (87.1%)
Type 2 DM, prevalence	15/19 (79.0%)	24/28 (85.7%)	35/45 (77.8%)	9/9 (100%)	83/101 (82.2%)
Time with DM, years	14.11 ± 8.30	13.64 ± 9.35	21.36 ± 9.62	23.33 ± 8.56	18.03 ± 9.92
HbA1C, %	6.26 ± 0.54	7.16 ± 0.85	7.43 ± 1.32	8.84 ± 1.87	7.26 ± 1.32
Insulin use, prevalence	3/19 (15.8%)	8/28 (28.6%)	30/45 (66.7%)	7/9 (77.8%)	48/101 (47.5%)
BCVA, logMAR	0.045 ± 0.069	0.020 ± 0.061	0.040 ± 0.087	0.189 ± 0.145	0.049 ± 0.094
IOP, mmHg	15.05 ± 2.25	14.89 ± 2.47	14.93 ± 3.34	15.33 ± 3.08	14.98 ± 2.87
SE, diopters	0.44 ± 1.82	–0.20 ± 2.26	0.19 ± 1.64	0.81 ± 1.00	0.19 ± 1.82

Data are presented as mean ± SD for continuous variables; and as count (relative frequency) for dichotomous variables

BCVA best-corrected visual acuity, *DM* diabetes mellitus, *HbA1c* glycosylated hemoglobin, *IOP* intraocular pressure, *logMAR* logarithm of the minimum angle of resolution, *SAH* systemic arterial hypertension, *SE* spherical equivalent

Table 2 Descriptive analysis of macular structural and vascular features on OCT/OCTA

	ETDRS stage				Total ($n = 101$)
	Level 10 ($n = 19$)	Level 20 ($n = 28$)	Level 35 ($n = 45$)	Levels 43/47 ($n = 9$)	
Structural outcomes					
GCC, µm	91.53 ± 8.63	95.21 ± 5.94	95.04 ± 8.41	95.11 ± 7.30	94.44 ± 7.77
Total retinal volume, mm^3	7.23 ± 0.43	7.20 ± 0.35	7.19 ± 0.41	7.29 ± 0.44	7.21 ± 0.40
Central retinal thickness, µm	231.47 ± 18.53	221.32 ± 12.21	239.51 ± 22.19	212.78 ± 28.58	230.57 ± 21.74
Parafoveal retina volume, mm^3	2.23 ± 0.12	2.20 ± 0.11	2.22 ± 0.13	2.18 ± 0.15	2.22 ± 0.12
Parafoveal retinal thickness, µm	321.68 ± 17.92	316.57 ± 17.38	318.38 ± 18.89	315.22 ± 21.12	318.22 ± 18.33
Vascular outcomes					
SCP total density, %	42.55 ± 4.62	45.25 ± 3.02	41.79 ± 3.80	39.70 ± 3.69	42.70 ± 4.09
SCP parafoveal density, %	45.29 ± 5.06	47.82 ± 3.36	44.04 ± 3.99	42.27 ± 4.50	45.16 ± 4.43
DCP total density, %	49.21 ± 3.29	51.10 ± 3.15	48.29 ± 3.55	43.38 ± 1.97	48.80 ± 3.84
DCP parafoveal density, %	51.43 ± 3.00	52.96 ± 3.02	49.82 ± 3.69	45.16 ± 2.33	50.58 3.89
FAZ area, mm^2	0.25 ± 0.10	0.23 ± 0.06	0.23 ± 0.09	0.30 ± 0.08	0.24 ± 0.09
CC density, %	47.70 ± 2.51	48.80 ± 4.70	46.70 ± 4.24	43.83 ± 5.34	47.21 ± 4.38

Data are presented as mean ± SD

CC choriocapillaris, *DCP* deep capillary plexus, *FAZ* foveal avascular zone, *GCC* ganglion cell complex, *SCP* superficial capillary plexus

arterial hypertension (OR = 3.82 (1.09, 13.41), $p = 0.037$), increasing time since diagnosis of DM (OR = 1.97 (1.32, 2.92), $p = 0.001$) and higher levels of HbA1c (OR = 2.20 (1.55, 3.12), $p < 0.001$) were all associated with higher risk of more-advanced NPDR, as expected.

Subsequently, the relevant predictors identified on univariate analysis were included in the multivariate model, which was used to build the final model, through a step-down procedure (as detailed in Methods). In both models, though, HbA1c level (OR = 2.48 (1.55, 3.95), $p < 0.001$) and DCP parafoveal density (OR = 0.54 (0.32, 0.92), $p = 0.024$) emerged as the most robust predictors of NPDR ETDRS Level. In order to test the goodness-of-fit of the final model, a Brant's test was performed; the result supports that the parallel regression assumption was not violated ($\chi^2 = 29.17$, $p = 0.404$, $df = 28$).

Representative scans of the DCP are shown in Fig. 2, highlighting the progressive capillary dropout in this plexus that occurs in the more-advanced stages of NPDR.

ROC curve analysis demonstrated that the final model has a relatively strong discriminative ability to differentiate DR stage at the main cutoff levels (10 vs. ≥ 20: C-statistic = 0.8770; ≤ 20 vs. ≥ 35: C-statistic = 0.8283; ≤ 35 vs. ≥ 43: C-statistic = 0.9527; Supplementary Figure 1).

Finally, as a sensitivity analysis, the same model building strategy was carried out on a clustered outcome (as in the

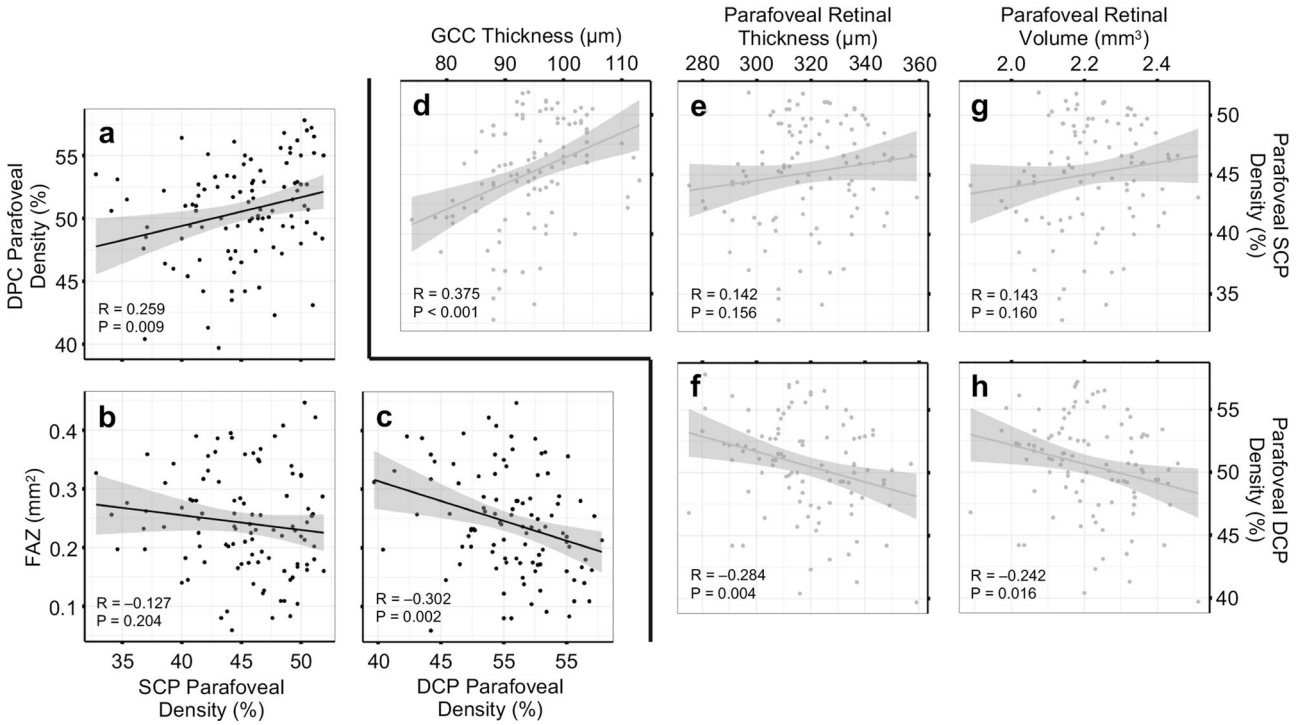

Fig. 1 Macular vascular–vascular and neuro-vascular correlations in diabetic patients. Scatter plots of correlations for vascular vs. vascular **a–c** and neuronal vs. vascular **d–h** OCTA parameters in diabetic patients. For each correlation, a regression line with a 95% CI (shaded area) was fitted. The regression coefficient (*R*) and its respective *P* value are indicated on each plot. DCP. Deep Capillary Plexus. FAZ. Foveal Avascular Area. GCC. Ganglion Cell Complex. SCP. Superficial Capillary Plexus

Table 3 Clinical and imaging predictors of NPDR ETDRS level

	Univariate model		Multivariate model		Final model	
	OR (95% CI)	*P*	OR (95% CI)	*P*	OR (95% CI)	*P*
Clinical features						
Age	1.01 (0.97, 1.05)	0.490				
SAH	3.82 (1.09, 13.41)	**0.037**	1.54 (0.25, 9.59)	0.642		
Time with DM[1]	1.97 (1.32, 2.92)	**0.001**	0.97 (0.55, 1.70)	0.914		
HbA1c	2.20 (1.55, 3.12)	**<0.001**	2.48 (1.35, 4.56)	**0.003**	2.48 (1.55, 3.95)	**<0.001**
Structural (OCT) measurements						
GCC	1.02 (0.96, 1.09)	0.488				
Total retinal volume[2]	1.00 (0.99, 1.01)	0.911				
Central retinal thickness	1.01 (0.98, 1.03)	0.600				
Parafoveal retinal volume[2]	0.99 (0.95, 1.02)	0.462				
Parafoveal retinal thickness	0.99 (0.97, 1.02)	0.578				
Vascular (OCTA) measurements						
SCP total density	0.87 (0.76, 0.99)	**0.033**	0.88 (0.28, 2.77)	0.822		
SCP parafoveal density	0.87 (0.76, 0.99)	**0.039**	1.00 (0.34, 2.92)	0.998		
DCP total density	0.81 (0.73, 0.89)	**<0.001**	1.92 (0.92, 3.97)	0.080	1.51 (0.88, 2.59)	0.138
DCP parafoveal density	0.79 (0.72, 0.87)	**<0.001**	0.43 (0.21, 0.89)	**0.023**	0.54 (0.32, 0.92)	**0.024**
FAZ area[3]	1.21 (0.63, 2.33)	0.570				
CC density	0.89 (0.80, 0.99)	**0.036**	0.94 (0.80, 1.10)	0.436	0.91 (0.80, 1.03)	0.119

[1] per 10 years increase; [2] per 0.01 mm^3 increase; [3] per 0.1 mm^2 increase

CC choriocapillaris, *DM* diabetes mellitus, *GCC* ganglion cell complex, *HbA1c* glycosylated hemoglobin, *OR* odds ratio, *SAH* systemic arterial hypertension

Statistically significant values are in bold $p < 0.05$

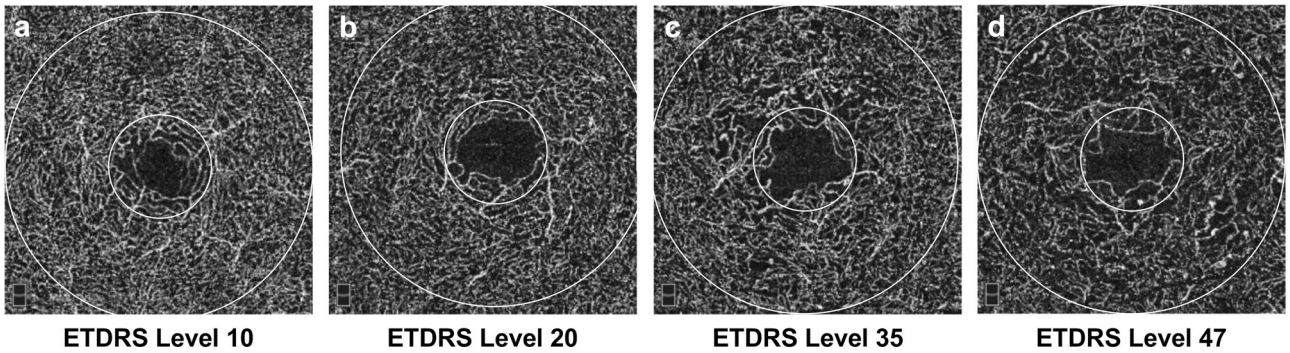

Fig. 2 Representative OCTA scans of the deep capillary plexus (DCP) for each main ETDRS stage. Representative 3 × 3 mm macular OCTA scans of the DCP of diabetic patients with DR staged at ETDRS Levels 10 **a**, 20 **b**, 35 C, **c** and 47 A **d**. These scans depict how the capillary density within the DCP decreases in more-advanced stages of NPDR

descriptive analysis); although there are slight variations in the values of the model parameters, the results completely overlap, suggesting that findings are robust to changes in outcome definition (Supplementary Table 1).

Discussion

We herein present a cross-sectional study of 101 eyes imaged with OCTA, in which the macular region was studied in order to ascertain whether any single or composite set of OCTA vascular measurements was able to predict ETDRS level—the gold-standard for DR grading—along the nonproliferative stages. Our results suggest that OCTA-based models may have a moderate-to-high ability to discriminate between the different stages of NPDR. Furthermore, in our analysis, parafoveal DCP vessel density was the OCTA parameter most robustly associated with NPDR ETDRS level.

On univariate analysis, several vascular OCTA parameters, but none of the structural OCT measurements studied, were found to be associated with ETDRS level, which suggests that OCTA may have superior capacity than OCT to detect changes associated with NPDR progression. While testing all relevant predictors on a multivariate model in order to control for confounding and select for robustness, the vascular density in the parafoveal DCP emerged as the only significant predictor.

Several studies have shown the usefulness of OCTA-based quantitative measurements for DR, using fractal dimensional analysis and area-based algorithms for vascular density and nonperfusion [7–9, 14–17]. Regarding the ability to detect DR, average fractal dimensions in both the SCP and DCP were shown to be lower for diabetic than in control eyes, although more significant differences were found in the DCP [9]. Accordingly, differences in the DCP were also shown to have higher index to discriminate diabetic from control patients [14]. Only one study suggested that vessel density in the SCP could have better discriminative ability to detect DR [18].

On the other hand, to differentiate NPDR from proliferative DR (PDR), (1) the fractal dimension of the DCP [7, 9], (2) local fractal analysis of the SCP [19], (3) parafoveal nonperfusion area analysis [15] and (4) vessel tortuosity analysis [16] were shown to be useful. However, differences within the NPDR spectrum (i.e., between mild and moderate–severe stages) were found neither in global fractal dimension [7] nor in vessel tortuosity analysis [18].

Our data add to these recently published studies by demonstrating that the parafoveal vessel density in the DCP seems to be the most robust OCTA parameter to differentiate clinical stages within the nonproliferative spectrum of DR. This is further supported by histological evidence that, in DR, vascular abnormalities are more pronounced in the DCP [20, 21]. Furthermore, it was recently shown that, among various OCTA parameters, vessel density in the DPC may have the strongest correlation with functional deficit [22]. Although the mechanism is unknown, one hypothesis suggests that the DPC may contribute more to the metabolic demands of photoreceptor metabolism in eyes with diabetic macular ischemia [23].

Furthermore, we found that FAZ area was not a significant predictor, even on univariate analysis (Table 3). This finding agrees with previous studies demonstrating that significant enlargement of FAZ occurs only at later stages, in the transition to PDR [16]. Indeed, although we found that both FAZ area and SCP vascular density were significantly correlated with parafoveal density in the DCP (Fig. 1), none of the former was found to be significant predictors of NPDR ETDRS level. Even if statistically significant, the coefficients indicate that these correlations are weak.

Overall, our data lend further support to the thesis that microvasculature quantifications with OCTA correlate with clinical observations. OCTA is non-invasive, quick to

perform, and reproducible for several retinal disorders [24]. Furthermore, scan segmentation is fully automated and, in this study, we used the vessel density measurements computed by the built-in software, thus circumventing the need for any computational-heavy or labor-intensive image analysis algorithms that, even if useful, have limited routine applicability.

This study was designed to evaluate progression along the nonproliferative stages; the purpose was not to test DR detection and, thus, non-diabetic patients were not included. The comparator in the analyses was the group of diabetic eyes on ETDRS Level 10. However, the predictive ability of some OCTA parameters may have been underestimated, as diabetic patients often manifest early microvascular retinal changes in the absence of clinically evident retinopathy [6, 25].

Moreover, there are important limitations to our study. First, the sample size is moderate at best, although within the same magnitude order of similar studies [6–9]. Second, this was a cross-sectional study; as we have no longitudinal data, we cannot describe how parafoveal DPC density changes over time. Third, OCTA has a small field of view and only parafoveal metrics were considered to detect NPDR progression. It is known that clinical signs of progression can be found in the peripheral retina, without macular involvement. OCTA also allows to analyze the peripapillary plexus; however, we have previously shown that capillary dropout in this plexus is likely not a suitable biomarker to detect NPRD progression [26].

Our study also has many strengths. Previous studies considered only mild vs. moderate–severe NPDR in their analysis [16, 19]. We used the gold-standard for DR staging —the ETDRS grading scheme—which allowed us to discriminate several intermediate stages, and thus to carefully confront clinical NPDR grading with OCTA measurements. Furthermore, our clinical evaluation was detailed, and careful statistical planning allowed to build valid models to test multiple predictors and adjust for potential confounding.

In summary, our study demonstrates that OCTA-based approaches can have a high discrimination index to differentiate between clinical substages within the NPDR spectrum. Furthermore, our data suggest that parafoveal vessel density in the DPC is the best single predictor to predict NPDR ETDRS level. In order to validate OCTA-based models for NPDR progression and, specifically, to validate parafoveal DCP density as a biomarker of NPDR progression, longitudinal studies are warranted.

Summary

What was known before

- Qualitative vascular abnormalities and quantitative measurements made with OCTA were shown to correlate with clinical features of DR: OCTA-based methods seem able to distinguish diabetic from non-diabetic patients, as well as to differentiate between the main clinical stages of DR (i.e., nonproliferative versus proliferative).

What this study adds

- An OCTA-based model has a moderate-to-high ability to discriminate between substages of DR, within the nonproliferative spectrum: the parafoveal vessel density of the deep capillary plexus was found to be the best single OCTA predictor of nonproliferative DR ETDRS level.

Acknowledgements We thank Brian L. Claggett, PhD (Cardiovascular Dept., Brigham and Women's Hospital, Boston, MA), for advice on the statistical analysis of this work.

Compliance with ethical standards

Conflict of interest None of the authors has any financial/conflicting interests to disclose.

References

1. Bourne RRA, Stevens GA, White RA, Smith JL, Flaxman SR, Price H, et al. Vision Loss Expert Group. Causes of vision loss worldwide, 1999–2010: a systematic analysis. Lancet Glob Health. 2013;1:e339–e349.
2. Zheng Y, He M, Congdon N. The worldwide epidemic of diabetic retinopathy. Indian J Ophthalmol. 2012;60:428–31.
3. Ferris FL. How effective are treatments for diabetic retinopathy? JAMA. 1993;269:1290–1.
4. Early Treatment Diabetic Retinopathy Study Research Group. Grading diabetic retinopathy form stereoscopic color fundus photographs – an extension of the modified airlie house classification. Ophthalmology. 1991;98:786–806.
5. Jia J, Tan O, Tokayer J, Potsaid B, Wang Y, Liu JJ, et al. Split-spectrum amplitude-decorrelation angiography with optical coherence tomography. Opt Express. 2012;20:4710–25.
6. Choi W, Waheed NK, Moult EM, Adhi M, Lee B, De Carlo T, et al. Ultrahigh speed swept source optical coherence tomography angiography of retinal and choriocapillaris alterations in diabetic patients with and without retinopathy. Retina. 2017;37:11–21.
7. Agemy S, Scripsema N, Shah C, Chui T, Garcia PM, Lee JG, et al. Retinal vascular perfusion density mapping using optical coherence angiography in normal and diabetic retinopathy patients. Retina. 2015;35:2353–63.
8. Kim AY, Chu Z, Shahidzadeh A, Wang RK, Puliafito CA, Kashani AH. Quantifying microvascular density and morphology in diabetic retinopathy using spectral-domain optical coherence tomography angiography. Invest Ophthalmol Vis Sci. 2016;57:OCT362–370.

9. Bhardwaj S, Tsui E, Zahid S, Young E, Mehta N, Agemy S, et al. Value of fractal analysis of optical coherence tomography angiography in various stages of diabetic retinopathy. Retina. 2018;38:1816–23.
10. Sandhu HS, Eladawi N, Elmogy M, Keynton R, Helmy O, Schaal S, et al. Automated diabetic retinopathy detection using optical coherence tomography angiography: a pilot study. Br J Ophthalmol. 2018;102:1564–69.
11. Kraus MF, Potsaid B, Mayer MA, Bock R, Baumann B, Liu JJ, et al. Motion correction in optical coherence tomography volumes on a per A-scan basis using orthogonal scan patterns. Biomed Opt Express. 2012;3:1182–99.
12. Nicolò M, Rosa R, Musetti D, Musolino M, Saccheggiani M, Traverso CE. Choroidal vacular flow area in central serous chorioretinopathy using swept-source coherence tomography angiograpvacular flow area in central serous chorioretinopathy using swept-source coherence tomography angiography. Invest Ophthalmol Vis Sci. 2017;58:2002–10.
13. Wickham, H ggplot2: Elegant Graphics for Data Analysis. Springer-Verlag New York, 2009.
14. Chen Q, Ma Q, Wu C, Tan F, Chen F, Wu Q, et al. Macular vascular fractal dimension in the deep capillary layer as an early indicator of microvascular loss for retinopathy in type 2 diabetic patients. Invest Ophthalmol Vis Sci. 2017;58:3785–94.
15. Krawitz BD, Phillips E, Bavier RD, Mo S, Carroll J, Rosen RB, et al. Parafoveal nonperfusion analysis in diabetic retinopathy using optical coherence tomography angiography. Transl Vis Sci Technol. 2018;7:4.
16. Lee H, Lee M, Chung H, Kim HC. Quantification of retinal vessel tortuosity in diabetic retinopathy using optical coherence tomography angiography. Retina. 2018;28:976–85.
17. Schottenhamml J, Moult EM, Ploner S, Lee B, Novais EA, Cole E, et al. An automatic, intercapillary area-based algorithm for quantifying diabetes-related capillary dropout using optical coherence tomography angiography. Retina. 2016;36: S93–S101.
18. Durbin MK, An L, Shemonski ND, Soares M, Santos T, Lopes M, et al. Quantification of retinal microvascular density in optical coherence tomographic angiography images in diabetic retinopathy. JAMA Ophthalmol. 2017;135:370–6.
19. Bhanushali D, Anegondi N, Gadde SG, Srinivasan P, Chidambara L, Yadav NK, et al. Linking retinal microvasculature features with severity of diabetic retinopathy using optical coherence tomography angiography. Invest Ophthalmol Vis Sci. 2016;57: OCT519–525.
20. Scarinci F, Nesper PL, Fawzi AA. Deep retinal capillary nonperfusion is associated with photoreceptor disruption in diabetic macular ischemia. Am J Ophthalmol. 2016;168:129–38.
21. Scarinci F, Jampol LM, Linsenmeier RA, Fawzi AA. Association of diabetic macular nonperfusion with outer retinal disruption on optical coherence tomography. JAMA Ophthalmol. 2015;133:1036–44.
22. Dupas B, Minvielle W, Bonnin S, Couturier A, Erginay A, Massin P, et al. Association between vessel density and visual acuity in patients with diabetic retinopathy and poorly controlled type 1 diabetes. JAMA Ophthalmol. 2018;136:721–8.
23. Cheung CMG, Wong TY. Clinical use of optical coherence tomography angiography in diabetic retinopathy treatment: ready for showtime? JAMA Ophthalmol. 2018;136/7:729–30.
24. Lee MW, Kim KM, Lim HB, Jo YJ, Kim JY. Repeatability of vessel density measurements using optical coherence tomography angiography in retinal diseases. Br J Ophthalmol. 2018b; pii: bjophthalmol-2018-312516.
25. De Carlo TE, Chin AT, Bonini Filho MA, Adhi M, Branchini L, Salz DA, et al. Detection of microvascular changes in eyes of patients with diabetes but not clinical diabetic retinopathy using optical coherence tomography angiography. Retina. 2015;35:2364–70.
26. Rodrigues TM, Marques JP, Soares M, Dolan MJ, Melo P, Simão S, et al. Peripapillary neurovascular coupling in the early stages of diabetic retinopathy. Retina. 2018. https://doi.org/10.1097/IAE.0000000000000232.